Tokai J Exp Clin Med., Vol. 29, No. 3, pp. 97-104, 2004

Design and its application of the f_n-ζ chart capable of direct readout of the highest frequency indicating the limit of obtaining distortion-free waveforms

Haruo FUKUYAMA, Yoshio KINEFUCHI*, Satoru SAITOH, Masahiro KANAZAWA, Masato SHIMADA*and Toshiyasu SUZUKI

Department of Anesthesiology, Tokai University School of Medicine
**Department of Biomedical Engineering, Tokai University School of High-Technology for Human Welfare*

(Received June 21, 2004; Accepted August 4, 2004)

We have already reported that the highest frequency (f_h) could serve as an index for evaluating the fidelity of pressure waveform derived via a catheter manometer system and be read off by the f_n-ζ chart. F_h is determined by the natural frequency (f_n) and damping coefficient (ζ) in the frequency characteristics of the system. Inversely, f_h determines two pairs of f_n and ζ in the f_n-ζ chart, one in the case of $\zeta < 0.7$ and the another $\zeta > 0.7$. Then, each pair of f_n and ζ determines respectively the resonant frequency (f_r) and its amplitude (A_r) ($\zeta < 0.7$), or the corner frequency (f_c) and its amplitude (A_c) ($\zeta > 0.7$) in the frequency characteristics. Thus, the point (f_r, A_r) or (f_c, A_c) represents the position of f_h projected in the frequency characteristics. Repeating the same operation for other f_n and ζ corresponding to the same f_h, yields the curve of f_h in the frequency characteristics. Calculations for other f_h's provide a group of curves. Frequency characteristics of pulmonary artery catheters were measured and overwritten thereupon, resulting in f_h's to be from 1.2 to 3.2 Hz. These results were in agreement with that calculated by the conventional method.

Key words : frequency characteristics, highest frequency (f_h), f_n-ζ chart, catheter manometer system

INTRODUCTION

Pressure waveforms via a catheter-manometer system may vigorously oscillate or be dulled and flattened. These are attributed to the cause that the frequency characteristics of the system involves a resonant peak or acts as a low-pass filter. In addition, these responses vary seriously depending on priming conditions of fluid. Clinically, it is of prime importance, therefore, to examine to what extent the pressure waveform is faithful and to explore how the fidelity may be improved.

As reported already, pressure waveforms mentioned above are evaluated by the highest frequency (f_h), i.e., the system can propagate the pressure waveform while keeping the distortion errors within a reasonable range, for example +/−5 % [1]. f_h is determined solely by the natural frequency (f_n) and damping coefficient (ζ) of the system. This process involves a somewhat complicated process.

In this paper, we introduced a method whereby f_h is directly read off graphically from the resonant peak or the corner point in the frequency characteristics of the system. In clinical use, this method would be an effective guide for improving the frequency characteristics.

THEORY

The general form of the second-order transfer function (G) is

$$G = 1/\{1-(\omega/\omega_n)^2 + j\{2\zeta(\omega/\omega_n)\} \quad (1)$$

where ω is angular frequency, ω_n represents

Haruo FUKUYAMA, Department of Anesthesiology, Tokai University School of Medicine, Bohseidai, Isehara, Kanagawa 259-1193, Japan TEL: 0463-93-1121 FAX: 0463-91-9260 E-mail: h-fuku@is.icc.u-tokai.ac.jp

natural angular frequency, j is imaginary number and ζ is damping coefficient [1, 2]. If the natural frequency is expressed as f_n, $\omega_n = 2\pi f_n$ [2-4]. The amplitude frequency characteristics may be given as the absolute (A) of Eq.(1):

$$A = 1/[\{1-(\omega/\omega_n)^2\}^2 + \{2\zeta(\omega/\omega_n)\}^2]^{1/2} \quad (2)$$

As obvious from Eq. (2), when $\zeta < 2^{-1/2}$, resonance (peak) exists in the amplitude frequency characteristics. If the frequency and amplitude at the resonance point are given as f_r and A_r, respectively, the equations:

$$f_n = f_r/(1-2\zeta^2)^{1/2} \quad (3)$$

$$\zeta^2 = [1-(1-1/A_r^2)^{1/2}] \quad (4)$$

hold between f_n and ζ [4, 5]. When $\zeta > 2^{-1/2}$, resonance does not exist in the amplitude frequency characteristics. In this instance, if the corner frequency (i.e., the point at which the log linear damping plot on the high frequency side intersects A = 1) is given as f_c and the amplitude at this point as A_c, the equations:

$$f_n = f_c \quad (5)$$

$$\zeta = 1/(2A_c) \quad (6)$$

hold between f_n and ζ [6, 7]. Figure 1 depicts the definition of f_r, A_r and f_c, A_c.

The f_n- ζ chart is presented in Figure 2. The area surrounded by 2 curves convex on left side and open on right side represents the combination range of f_n and ζ to obtain f_h (1). The pair of f_n and ζ calculated from Eqs. 3 and 4 or from Eqs. 5 and 6 corresponds to the point (f_n, ζ) on the chart and gives the highest frequency (f_h). As can be seen from the chart, fn have two f_h's corresponding to the domain of $\zeta < 2^{-1/2}$ (i.e., $\zeta < 0.7$ approx.) in the case of Eqs. 3 and 4, or to the domain of $\zeta > 2^{-1/2}$ in the case of Eqs. 5 and 6, respectively.

For each domain in the f_n- ζ chart, the pair of f_n and ζ on the curve of f_h is read off. Then, in the case of $\zeta < 0.7$, f_r and A_r are inversely calculated by substituting the pair of fn and ζ into Eqs. 3 and 4, that is, these equations are rewritten as follows;

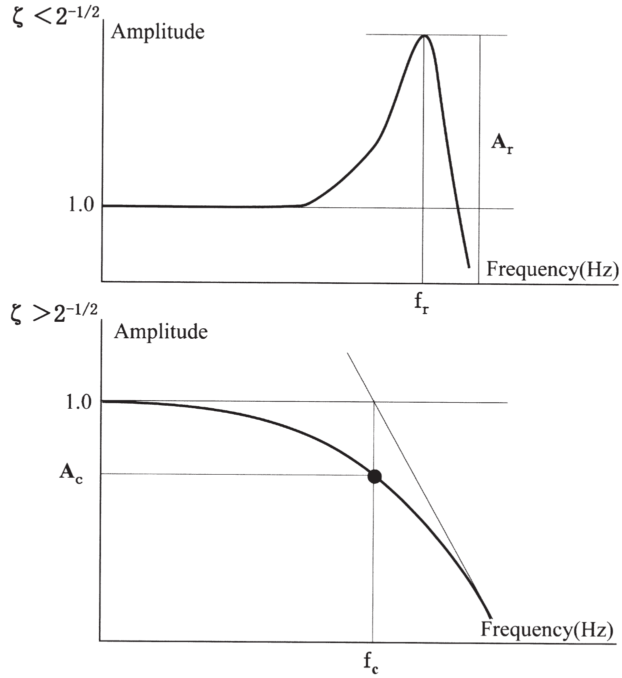

Fig. 1 Definition of f_r, A_r, and f_c, A_c. The ordinate represents the output/input amplitudes ratio. The abscissa means the frequency. When $\zeta < 2^{-1/2}$, resonant peak exists in the frequency characteristics, and the frequency and amplitude at that point are referred as f_r and A_r. They determine f_n and ζ by Eqs. 3 and 4. When $\zeta > 2^{-1/2}$, resonance does not exist. In this case, the frequency and amplitude at that point the log linear damping line (approximately -12dB/oct.) intersects Amplitude = 1 are referred as f_c and A_c. They determine f_n and ζ by Eqs. 5 and 6.

$$f_r = f_n(1 - 2\zeta^2)^{1/2} \quad (7)$$

$$A_r^2 = 1/[1 - (1 - \zeta^2)^2] \quad (8)$$

Similarly, in the case of $\zeta > 0.7$, f_c and A_c are calculated by substituting the pair of f_n and ζ into Eqs. 5 and 6, that is, these equations are also rewritten as follows:

$$f_c = f_n \quad (9)$$

$$A_c = 1/(2\zeta) \quad (10)$$

The points (f_r, A_r) and/or (f_c, A_c) give the position of f_h projected in the amplitude frequency characteristics. Repeating the same operation for other pair of f_n and ζ on the same curve of f_h yields a set of curves corresponding to f_h. Figure 3 shows results for all f_h values. The area surrounded 2 curves convex on left side with the blank area of $0.7 < \zeta < 1$ represents the range of f_h in the frequency characteristics. When the frequency characteristics of a catheter-manometer system are plotted on this chart, the position of the resonant peak (in the case of $\zeta < 0.7$) or corner point (in the case of

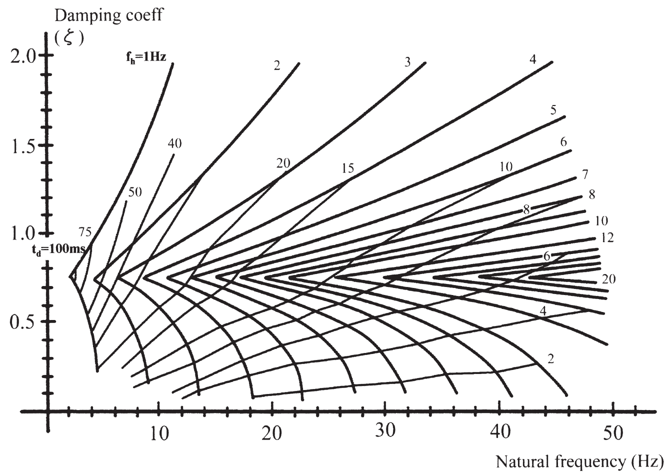

Fig. 2 f_n-ζ chart. The ordinate represents ζ and the abscissa f_n. The area surrounded by 2 curves convex on left side and open on right side represents the combination range of f_n and ζ to obtain f_h. The curves named t_d mean the propagation delay time through a catheter. By plotting measured f_n and ζ on the chart, the highest frequency (f_h) and the propagation delay time (t_d) can be determined.

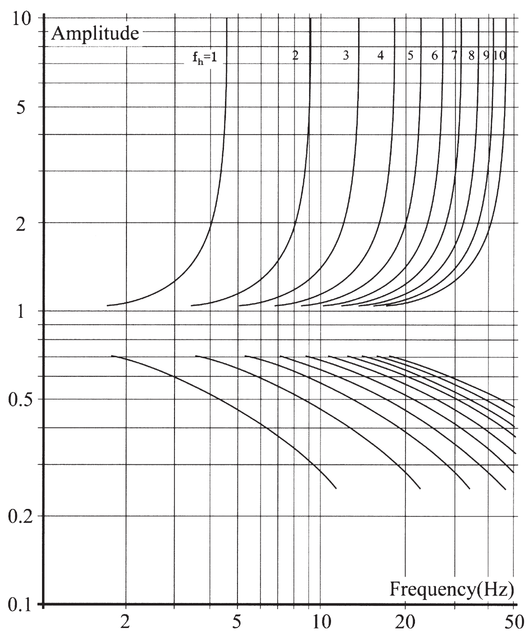

Fig. 3 F_h chart. The area surrounded 2 curves convex on left side with the blank area of $0.7 < \zeta < 1$ represents the position of (f_r, A_r) and/or (f_c, A_c) corresponding to f_h. By plotting the resonance point or corner point thereof provides f_h of the system. Theoretically, no resonance point or corner point is positioned in the blank area.

$\zeta > 0.7$) thereof provides f_h of that system. The area defined by $0.7 < \zeta < 1$ in the chart is blank. Theoretically, no resonant peak or corner point is positioned in this area. Figure 3 is referred to as the F_h chart. The relationship between the F_h chart and the f_n-ζ chart is demonstrated graphically in the appendix.

METHODS

To verify the above-suggested theory and corroborate the F_h chart, frequency characteristics of pulmonary artery catheters were measured. Details of the method to measure frequency characteristics are described elsewhere [1, 2, 8]. A pulmonary artery catheter (407, B. Braun, USA) filled with lactated Ringer solution served as a subject. The measurement was carried out on three priming conditions of lactated Ringer solution, i.e., (1) degassed with a vacuum pump at room temperature, (2) simply maintained at room temperature, and (3) heated to 37 °C after priming at room temperature.

Where resonance was observed in the frequency characteristics, f_r and A_r were determined, followed by calculation of f_n and ζ using Eqs. 3 and 4. If resonance wasn't observed, f_n and ζ were calculated directly from the Nyquist diagram in order to avoid inaccuracy in determining f_c and A_c. Of course, in this case, the phase frequency characteristics were measured simultaneously [2, 6, 7]. Values obtained thereby for f_n and ζ were plotted on the f_n- ζ chart, to read off f_h values.

The obtained three frequency characteristics were overwritten on Figure 3, so that f_h values were read out from the position of resonance point or corner point and compared with the values obtained from the f_n-ζ chart mentioned above.

RESULTS

Frequency characteristics were illustrated in Figure 4. They were obtained on three different priming conditions of lactated Ringer solution as mentioned above, that is, (1) degassed with a vacuum pump at room temperature, (2) simply maintained at room temperature, and (3) heated to 37 °C after

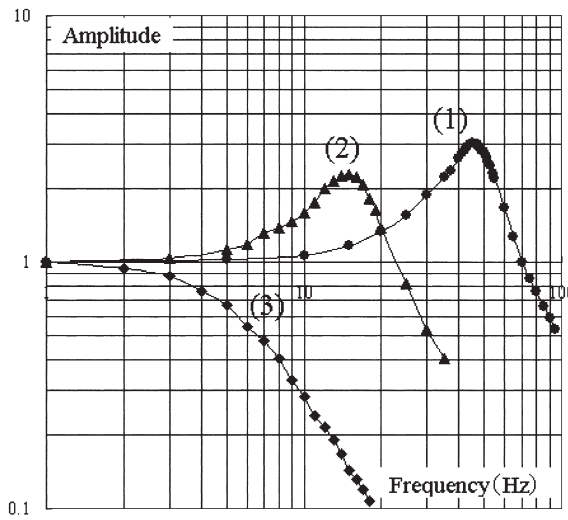

Fig. 4 Frequency characteristics of a pulmonary artery catheter. The curves correspond to three different priming conditions, i.e., lactated Ringer solution was (1) degassed with a vacuum pump at room temperature, (2) simply maintained at room temperature, and (3) heated to 37 °C after filling at room temperature. In the cases of (1) and (2), f_n and ζ were calculated using Eqs. 3 and 4 as there was an obvious resonance, resulting in f_n = 45.3 Hz, ζ = 0.17 and f_n = 15.8 Hz, ζ = 0.23 respectively, while, in the case of (3), f_n and ζ were calculated from the Nyquist diagram since the frequency characteristics did not have resonance. The Nyquist diagram obtained was omitted here. Results were f_n = 5.0 Hz, ζ = 0.76.

priming at room temperature. In the cases of (1) and (2), f_n and ζ were calculated using Eqs. 3 and 4 as there was an obvious resonance, resulting in f_n = 45.3 Hz, ζ = 0.17 and f_n = 15.8 Hz, ζ = 0.23 respectively, while, in the case of (3), f_n and ζ were calculated from the Nyquist diagram since the frequency characteristics did not have resonance. The Nyquist diagram obtained was omitted here. Results were f_n = 5.0 Hz, ζ = 0.76. By plotting these values on the f_n- ζ chart, Figure 5 was obtained, showing f_h's ranging from 2.1 Hz to 10.3 Hz. In addition to the latter case, as depicted in the figure, the measurement was carried out up to amplitude damping to nearly 1/10 in order to determine the linear decay plot on the higher frequency side, resulting in f_c = 4.8 Hz, A_c = 0.67.

The three frequency characteristics shown in Figure 5 were overwritten on the F_h chart, and presented in Figure 6. The f_h values at the resonance points for the case of (1) and

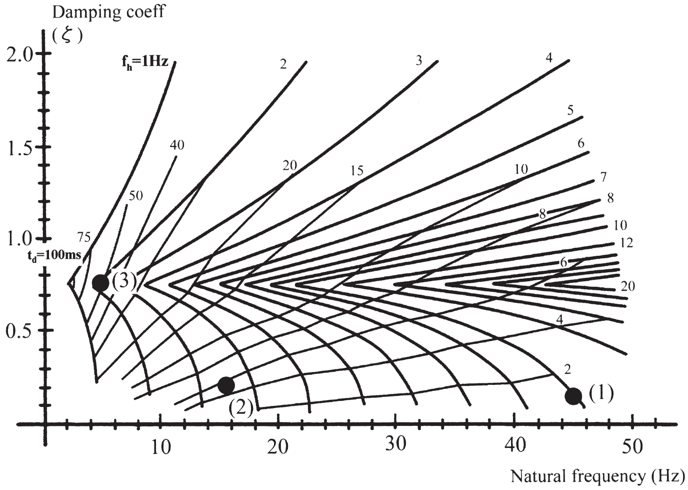

Fig. 5 Determination of f_h's in the f_n- ζ chart. The points on the chart represent the combinations of f_n and ζ corresponding to three priming conditions shown in Fig. 4. The f_h values at the resonance points for the case of (1) and (2) and at the corner point for the case of (3) were 10.2, 3.5 and 2.1 Hz

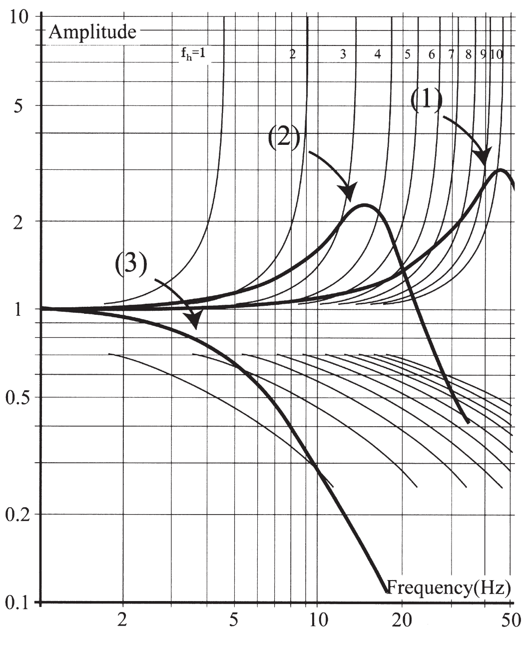

Fig. 6 Determination of f_h's in the F_h chart. The f_h's at the resonance peaks observed in the characteristics (1) and (2) were 10.2 Hz and 3.5 Hz, respectively, and at the corner point observed in the characteristics (3), f_h was read off as 2.1 Hz.

(2) and at the corner point for the case of (3) were 10.2, 3.5 and 2.1 Hz, respectively. These data were in agreement with the f_h values calculated from the frequency characteristics mentioned above.

DISCUSSION

Waveform distortions obtained via a catheter-manometer system are composed of two elements, namely the difference in amplitude and phase lag [1-3]. We have proposed to define these distortions quantitatively by solving a second order kinetic equation and to plot them on a chart composed of three parameters, f_n ζ , and f_h. It has become feasible with the chart to quantitatively evaluate the degree of waveform distortion derived via a catheter-manometer system. This chart was referred to as the f_n-ζ chart.

On evaluating waveforms in the f_n- ζ chart, it is required to measure f_n and ζ of the catheter-manometer system. From the clinical viewpoint, f_n and ζ can be calculated from the transient phenomenon that occurs on flushing or forced tapping the catheter-manometer system [5, 9, 10]. These techniques are quite useful as they permit measurement of f_n and ζ during clinically monitoring status. Yet, they have a drawback of being somewhat deficient in reproducibility due to instability of transient phenomenon [8, 11]. From the practical viewpoint, calculation of f_n and ζ from Eqs. 3 and 4 after measurement of the frequency characteristics is the most accurate procedure in designing a catheter-manometer system as well as in assessing the construction scheme for the system.

In this paper, we described the method for determining f_h directly from the measured frequency characteristics. This method is non-cumbersome and is even visually comprehensive as the position of the resonance point corresponds to the highest frequency per se. Furthermore, a burden for software may be substantially reduced in case of designing a waveform evaluation device using this method. In the instance where resonance is not involved, the method may also be applied in the same manner insofar as the position of the corner frequency is determined. Determination of the linear damping plot on the high frequency side is prone to lead to an error in this instance, but the evaluation of the system itself has no much meaning. It would be well enough to take it as an effective guide for improving the frequency characteristics.

The chart named "Gabarith window" has been introduced as a method for determining the quality of frequency characteristics [11], wherein the degree of fidelity of derived waveforms is assessed with 2, 5 and 10 % limits of error displayed on the amplitude frequency characteristics. The chart seems to be constructed on the following rationale. Based on the mean value and its variation in the power-spectral distributions of directly derived pressure waveforms from patients, and with multiplying them the prescribed error rates, the distribution limits of frequency characteristics were constructed. But, this still is nothing more than an inference because the process of constructing the chart has not been disclosed. Whatever the process, the chart doesn't pay any attention to the resonant peak, so that it cannot discriminate the direction for improving the frequency characteristics. However, the demarcations of areas in the chart are similar partially to our F_h chart. In other words, it may be said that our chart has proven the "Gabarith window" theoretically.

Taking into consideration the discussion up to now, we would like then to mention about a method to improve the frequency characteristics. Suppression of a resonance peak using a damping device may be undertaken on the rationale that the flattened frequency characteristics permits the waveform to be faithful [12, 13]. This approach entails the decrease in f_n and the increase in ζ to be adjusted near to 0.7. With decreasing f_n, f_h decreases as shown in the F_h chart, and also with increasing ζ , the delay time of derived pressure waveform increases as illustrated in the f_n-ζ chart, so that timing with other vital signs such as ECG may fail. It is thus by no means a recommendable method. Such problem will not arise if frequency characteristics are rendered flat within the frequency bandwidth of pressure waveform, by shifting the resonance point to the outside of the higher frequency side. Clinically, reconstructing of the system including the priming procedure can cope with this problem.

APPENDIX

The graphical procedures allow the derivation of the F_h chart to be grasped easily. In

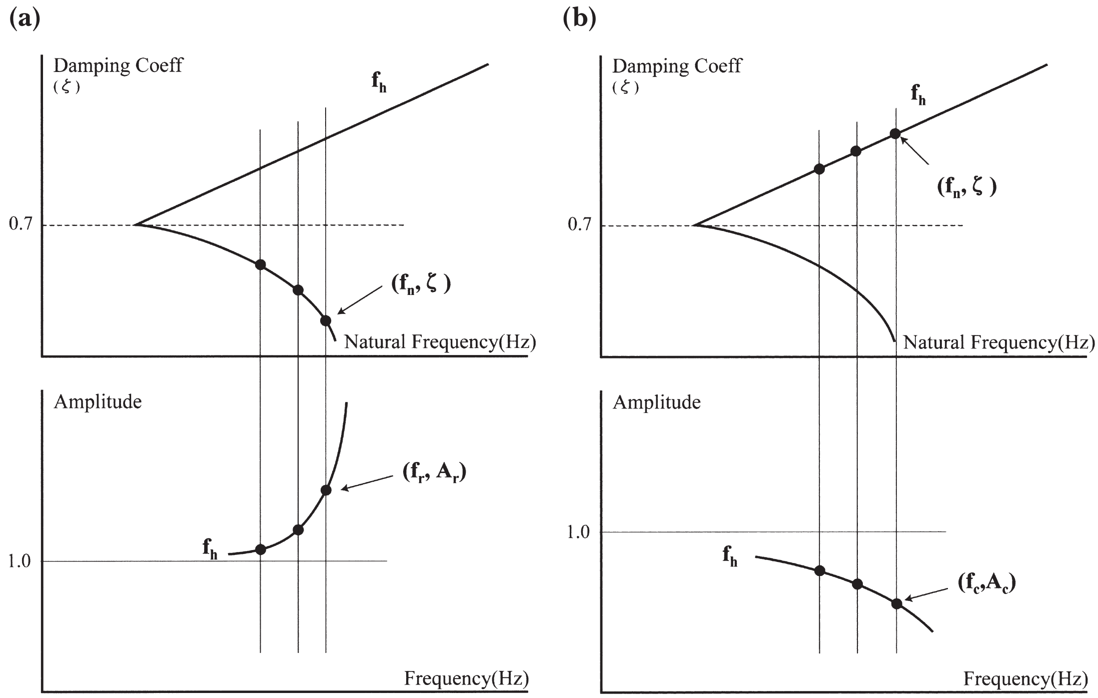

Fig. 7 Relationship between f_n-ζ chart and F_h chart. In the figure (a), the upper portion shows the pair of f_n and ζ corresponding to f_h in the f_n-ζ chart, and the lower portion shows the pair of f_r and A_r calculated from Eqs. 7 and 8. The pair of f_r and A_r has the same coordinate system as that of the frequency characteristics. This means that f_h in the f_n-ζ chart is projected in the frequency characteristics. Similar process is shown in the figure (b). In the figure, the lower portion shows the pair of f_c and A_c calculated from Eqs. 9 and 10. In this case, f_h is projected on the point (f_c, A_c).

the case of $\zeta < 0.7$, Figure 7 (a) shows the relationship between Figure 2 (i.e., f_n- ζ chart) and Eqs. 7 and 8. In the figure, the upper portion shows the pair of f_n and ζ corresponding to f_h, and the lower portion shows the pair of f_r and A_r calculated from Eqs. 7 and 8. As a result, f_h is projected on the point (f_r, A_r) which is on the same coordinate system as that of the frequency characteristics. Repeating the same operations for other pairs of f_n and ζ make a curve of f_h in the frequency characteristics. In the case of $\zeta >$ 0.7, similar process is shown in Figure 7(b). In the figure, the lower portion shows the pair of f_c and A_c calculated from Eqs. 9 and 10. In this case, f_h is projected on the point (f_c, A_c).

REFERENCES

1) Kinefuchi Y, Suzuki T, Takiguchi M, Yamasaki Y, Yamamoto Y.: Evaluation of dynamic response of catheter-manometer system for pulmonary arterial pressure. J Appl Physiol 77: 2023-2028, 1994.
2) Milhorn HT.: The application of control theory to physiological systems. Philadelphia, WB Saunders, 1966.
3) Fry DL.: Physiologic recording by modern instruments with particular reference to pressure recording. Physiol Rev 40: 753-788, 1960.
4) Gersh BJ.: Measurement of intravascular pressures, The circulation in anaesthesia : Applied physiology and pharmacology. Edited by Prys-Roberts C. Oxford, Blackwell Scientific Publications, pp 511-518, 1980.
5) Hipkins SF, Rutten AJ, Runciman WB.: Experimental analysis of catheter-manometer systems *in vitro* and *in vivo*. Anesthesiology 71: 893-906, 1989.
6) Milhorn HT.: Transient analysis of physical systems, The application of control theory to physiological systems. Philadelphia, WB Saunders, pp 78-93, 1966.
7) Geddes LA.: Direct measurement of blood pressure. In: The direct and indirect measurement of blood pressure. Chicago, IL, Year Book Medical, pp 47-69, 1970.
8) Kinefuchi Y, Suzuki T, Takiguchi M, Yamasaki Y, Yamamoto M, Suwa M.: Natural frequency/damping coefficient relationship of the catheter-manometer

system required for high-fidelity measurement of the pulmonary arterial pressure. J Anesthesia 7: 419-426, 1993.

9) Glantz SA, Tyberg JV.: Determination of frequency response from step response: application to fluid-filled catheters. Am J Physiol 236: H376-H378, 1979.
10) Kinefuchi Y, Fukuyama H, Saitoh S, Kanazawa M, Takiguchi M.: Evaluation of pulmonary artery pressure waveforms using catheter-manometer system in clinical use (in Japanese with English abstract). J J Circ Cont 23: 24-30, 2002.
11) Billiet E, Colardyn F.: Hazardous information from bedside fast flush device test for fluid-filled pressure monitoring system. Angiology 71: 893-906, 1989.
12) Gardner RM.: Direct blood pressure measurement-dynamic response requirements. Anesthesiology 54: 227-236, 1981.
13) Rutten AJ, Nancarrow C, Ilsley AH, Runciman WB.: An assessment of six different pulmonary artery catheters. Crit Care Med 15: 250-255, 1987.